Important Notice to Authors

No further publication processing will occur until we receive your response to this proof.

Attached is a PDF proof of your forthcoming article in *Physical Review Letters*. The article accession code is LH16229.

Your paper will be in the following section of the journal: LETTERS — Condensed Matter: Electronic Properties, etc.

Please note that as part of the production process, APS converts all articles, regardless of their original source, into standardized XML that in turn is used to create the PDF and online versions of the article as well as to populate third-party systems such as Portico, Crossref, and Web of Science. We share our authors' high expectations for the fidelity of the conversion into XML and for the accuracy and appearance of the final, formatted PDF. This process works exceptionally well for the vast majority of articles; however, please check carefully all key elements of your PDF proof, particularly any equations or tables.

Figures submitted electronically as separate files containing color appear in color in the online journal.
However, all figures will appear as grayscale images in the print journal unless the color figure charges have been paid in advance, in accordance with our policy for color in print (https://journals.aps.org/authors/color-figures-print).

Specific Questions and Comments to Address for This Paper

The numbered items below correspond to numbers in the margin of the proof pages pinpointing the source of the question and/or comment. The numbers will be removed from the margins prior to publication.

1 Please check and clarify whether “Moscow distr.” in affiliation 3 should be kept simply as “Moscow” or “Moscow District.”

2 Except for the term “and/or," the use of the slash is discouraged between words and abbreviations, as the intent of the solidus is ambiguous. Several possibilities for its meaning exist, among them “and," “or," “and/or," and “plus." We ask that more precise, and therefore more meaningful, conjunctions be used. For terms that are diagrammatically opposed, we use a hyphen (e.g., liquid-solid interface, vacancy-acceptor interface). Please check the replacements in the sentence beginning “The contact angle is the same" and similar changes of the slash throughout. Thank you.

3 Please see the APS memo at http://journals.aps.org/authors/multiplication-signs-h11 for using multiplication sign in equations, and suggest whether the multiplication sign in Eq. (1) and throughout should be removed.

4 Please review the funding information section of the proof's cover letter and respond as appropriate. We must receive confirmation that the funding agencies have been properly identified before the article can publish.

5 NOTE: External links, which appear as blue text in the reference section, are created for any reference where a Digital Object Identifier (DOI) can be found. Please confirm that the links created in this PDF proof, which can be checked by clicking on the blue text, direct the reader to the correct references online. If there is an error, correct the information in the reference or supply the correct DOI for the reference. If no correction can be made or the correct DOI cannot be supplied, the link will be removed.

6 A check of online databases revealed a possible error in Ref. [8]. The page number has been changed from '104407' to '014407'. Please confirm this is correct.

7 Please send a brief description of the supplemental material to be included in the required reference. The URL link will be activated at the time of publication.

8 A check of online databases revealed a possible error in Ref. [29]. The volume has been changed from '90' to '94'. Please confirm this is correct.

9 A check of online databases revealed a possible error in Ref. [37]. The year has been changed from '2014' to '2015'. Please confirm this is correct.

Titles in References

The editors now encourage insertion of article titles in references to journal articles and e-prints. This format is optional, but if chosen, authors should provide titles for *all* eligible references. If article titles remain missing from eligible references, the production team will remove the existing titles at final proof stage.

Funding Information

Information about an article's funding sources is now submitted to Crossref to help you comply with current or future funding agency mandates. Crossref's Open Funder Registry (https://www.crossref.org/services/funder-registry/) is the definitive registry of funding agencies. Please ensure that your acknowledgments include all sources of funding for your article following any requirements of your funding sources. Where possible, please include grant and award ids. Please carefully check the following funder information we have already extracted from your article and ensure its accuracy and completeness:

- U.S. Department of Energy, FundRef ID http://dx.doi.org/10.13039/100000015 (United States/US)
- Basic Energy Sciences, FundRef ID http://dx.doi.org/10.13039/100006151 (United States/US)
- Microelectronics Advanced Research Corporation, FundRef ID http://dx.doi.org/10.13039/100007245 (United States/US)
- Defense Advanced Research Projects Agency, FundRef ID http://dx.doi.org/10.13039/100000185 (United States/US)

Other Items to Check

- Please note that the original manuscript has been converted to XML prior to the creation of the PDF proof, as described above. Please carefully check all key elements of the paper, particularly the equations and tabular data.
- Title: Please check; be mindful that the title may have been changed during the peer-review process.
- Author list: Please make sure all authors are presented, in the appropriate order, and that all names are spelled correctly.
- Please make sure you have inserted a byline footnote containing the email address for the corresponding author, if desired. Please note that this is not inserted automatically by this journal.
- Affiliations: Please check to be sure the institution names are spelled correctly and attributed to the appropriate author(s).
- Receipt date: Please confirm accuracy.
- Acknowledgments: Please be sure to appropriately acknowledge all funding sources.
- References: Please check to ensure that titles are given as appropriate.
- Hyphenation: Please note hyphens may have been inserted in word pairs that function as adjectives when they occur before a noun, as in “x-ray diffraction,” “4-mm-long gas cell,” and “*R*-matrix theory.” However, hyphens are deleted from word pairs when they are not used as adjectives before nouns, as in “emission by x rays,” “was 4 mm in length,” and “the *R* matrix is tested.”
  Note also that Physical Review follows U.S. English guidelines in that hyphens are not used after prefixes or before suffixes: superresolution, quasiequilibrium, nanoprecipitates, resonancelike, clockwise.
- Please check that your figures are accurate and sized properly. Make sure all labeling is sufficiently legible. Figure quality in this proof is representative of the quality to be used in the online journal. To achieve manageable file size for online delivery, some compression and downsampling of figures may have occurred. Fine details may have become somewhat fuzzy, especially in color figures. The print journal uses files of higher resolution and therefore details may be sharper in print. Figures to be published in color online will appear in color on these proofs if viewed on a color monitor or printed on a color printer.
- Overall, please proofread the entire *formatted* article very carefully. The redlined PDF should be used as a guide to see changes that were made during copyediting. However, note that some changes to math and/or layout may not be indicated.

Ways to Respond

- ***Web:*** If you accessed this proof online, follow the instructions on the web page to submit corrections.
- ***Email:*** Send corrections to aps-robot@luminad.com. Include the accession code LH16229 in the subject line.
- ***Fax:*** Return this proof with corrections to +1.855.808.3897.

If You Need to Call Us

You may leave a voicemail message at +1.855.808.3897. Please reference the accession code and the first author of your article in your voicemail message. We will respond to you via email.

Response to specific questions and comments:

1. Change to 'Institute for Solid Physics, RAS, Chernogolovka, 142432, Russia'
2. In 'HM/FM/I' the dash is used to describe layered structure, from bottom to top is HM, FM and I.
3. We need keep the multiplication 'X' here, which means the vector product.
4. Grant numbers were confirmed to be right.
4. Please add "Q. M. Thanks Yue Zhang for micromagnetic simulation" in acknowledgment.
5. We have confirmed.
6. Confirmed
7. .... for SOT switching in W/CoFeB/MgO (I), and asymmetric domain wall expansion (II, III, IV).
8. Confirmed
9. Confirmed.

Other corrections:

1. Figure 3b should be ABCDE, (old one is ABCDD). Corrected

Switching a Perpendicular Ferromagnetic Layer by Competing Spin Currents

Qinli Ma,[1,*] Yufan Li,[1] D. B. Gopman,[2] Yu. P. Kabanov,[2,3] R. D. Shull,[2] and C. L. Chien[1,†]
[1]*Department of Physics and Astronomy, Johns Hopkins University, Baltimore, Maryland 21218, USA*
[2]*National Institute of Standards and Technology, Gaithersburg, Maryland 20899, USA*
[3]*Institute for Solid State Physics, RAS, Chernogolovka, Moscow distr., 142432, Russia*

(Received 24 August 2017)

An ultimate goal of spintronics is to control magnetism via electrical means. One promising way is to utilize a current-induced spin-orbit torque (SOT) originating from the strong spin-orbit coupling in heavy metals and their interfaces to switch a single perpendicularly magnetized ferromagnetic layer at room temperature. However, experimental realization of SOT switching to date requires an additional in-plane magnetic field, or other more complex measures, thus severely limiting its prospects. Here we present a novel structure consisting of two heavy metals that delivers competing spin currents of opposite spin indices. Instead of just canceling the pure spin current and the associated SOTs as one expects and corroborated by the widely accepted SOTs, such devices manifest the ability to switch the perpendicular CoFeB magnetization solely with an in-plane current without any magnetic field. Magnetic domain imaging reveals selective asymmetrical domain wall motion under a current. Our discovery not only paves the way for the application of SOT in nonvolatile technologies, but also poses questions on the underlying mechanism of the commonly believed SOT-induced switching phenomenon.

DOI:

Switching of ferromagnets is central to many magnetic memory applications from high-density magnetic recording to magnetic random access memories (MRAM) [1,2]. A ferromagnetic (FM) entity can always be, and for a long time could only be, switched by a magnetic field. The discovery of spin transfer torque (STT) enabled current switching of FM entities in nanostructures, whereby spin polarized currents generated in a pinned FM layer in a FM-metal-FM (spin valve) or FM-insulator-FM (magnetic tunnel junction) device exerts a torque on the magnetization of a second (free) FM layer [3–6]. However, the high STT switching current density through the device is undesirable.

The advent of spin-orbit torque (SOT) allows the prospects of electrical switching of a single FM layer with perpendicular magnetic anisotropy (PMA) by a peripheral current [7–12]. The general structure of a perpendicular SOT device is a HM/FM/I trilayer, as shown in Fig. 1(a), where the FM layer (e.g., Co, CoFeB), sandwiched between a heavy metal (HM), e.g., Pt and W, and a light oxide (I), e.g., AlO_x and MgO, acquires PMA. Because of the spin Hall effect (SHE) and the interfacial Rashba effect, a charge current $\boldsymbol{J}$ (in the x direction) gives rise to a pure spin current $\boldsymbol{J}_s \propto \theta_{SH}\boldsymbol{J}\times\boldsymbol{\sigma}$ and a spin accumulation in the out-of-plane (z) direction, respectively, with a spin index $\boldsymbol{\sigma}$ in the direction perpendicular to both $\boldsymbol{J}_s$ and $\boldsymbol{J}$, that is along the y direction [7–9]. The effective spin Hall angle θ_{SH} specifies the charge-to-spin conversion efficiency. Heavy metals with large θ_{SH}, such as Pt, Ta, and W [10–14], are important for SOT devices, in which the anomalous Hall effect (AHE) generates a transverse voltage in proportion to the orientation of the perpendicularly magnetized layer [Fig. 1(b)]. As illustrated in Fig. 1(a) and in contrast to STT devices, the charge current passes peripheral to, and not through, the magnetic multilayers.

Switching of a PMA layer by SOT was first demonstrated by Miron *et al.* in 2011 and Liu *et al.* in 2012 in $Pt/Co/AlO_x$ [10,11]. We have obtained similar results in W/CoFeB/MgO (See Supplementary Material I [15] for SOT switching in W/CoFeB/MgO). However, to date, SOT switching in HM/FM/I multilayers cannot occur

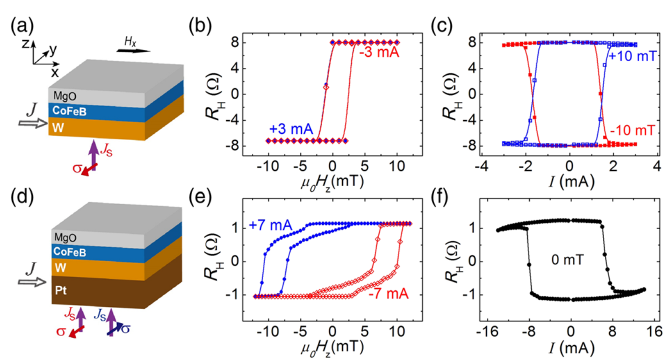

FIG. 1. Structures and current-induced switching behaviors in CoFeB with PMA, patterned with $\alpha = 0°$. (a) Conventional SOT switching in W(1)/CoFeB(1)/MgO(1.8), (b) anomalous Hall effect (AHE) effect under +3 mA (blue solid circles) and −3 mA (open diamond circles), and (c) switching requiring a magnetic field. (d) Competing SOT effects of Pt/W/CoFeB/MgO. (e) AHE under positive and negative current. (f) Current induced magnetization switching requiring no magnetic field.

unless an external magnetic field $\mu_0\boldsymbol{H}_x$ is also applied along the current direction. The field direction, parallel or antiparallel to $\boldsymbol{J}$, dictates the states with up or down magnetization at large current. [Fig. 1(c)]. Higher $\mu_0\boldsymbol{H}_x$ reduces the switching current density, but switching cannot occur at any current density without a magnetic field. The requirement of a magnetic field severely diminishes the prospects of SOT switching. By altering the anisotropy of the FM layer, using an asymmetrical geometrical shape or magnetic exchange bias, switching without a field has been demonstrated in prototype devices [16–20], but scaling these measures up for technologically relevant device arrays may present unique challenges.

Present understanding of SOT switching in HM/FM/I is based on the Dzyaloshinskii-Moriya interaction (DMI) and the domain wall (DW) motion driven by SOT [21–26]. The DMI at the HM/FM interface causes a Néel DW with a certain chirality. For a series of hypothetical up ($\uparrow$)/down($\downarrow$) domains along the x direction with magnetization pointing in the $+z/-z$ directions, spins within the DWs rotate in the vertical xz plane with a single chirality that is set by the sign of the DMI constant. Under a current in the x direction, the SOT causes motion of the DW. Theoretical and experimental studies in the last few years have concluded that the relevant SOT for HM/FM/I, has two terms, namely, the fieldlike torque $\boldsymbol{\tau}_{FL} = a\boldsymbol{M}\times\boldsymbol{\sigma}$ and the anti-damping-like torque $\boldsymbol{\tau}_{\mathbf{DL}} = b\boldsymbol{M}\times(\boldsymbol{\sigma}\times\boldsymbol{M})$, where mainly the latter drives the DWs [21–24]. The Landau-Lifshitz-Gilbert (LLG) equation including the SOT is

$$\frac{\partial \boldsymbol{M}}{\partial t} = -\gamma\boldsymbol{M}\times H + \frac{\alpha}{M}\boldsymbol{M}\times\frac{\partial \boldsymbol{M}}{\partial t} + a\boldsymbol{M}\times\boldsymbol{\sigma} + b\boldsymbol{M} \times(\boldsymbol{\sigma}\times\boldsymbol{M}), \quad (1)$$

where the first two terms are the precession term and the damping term. The corresponding effective fields of the two terms of SOT, $\boldsymbol{H}_{\mathbf{FL}}\sim\boldsymbol{\sigma}$ and $\boldsymbol{H}_{\mathbf{DL}}\sim\boldsymbol{\sigma}\times\boldsymbol{M}$ are in the xy plane along the y and the x axes, respectively, shown in Fig. 1(a). For DWs with one chirality, the effective field $\boldsymbol{H}_{\mathbf{DL}}$ acting on the $\uparrow\downarrow$ and $\downarrow\uparrow$ DWs are also opposite. Consequently, the SOTs influence both $\uparrow\downarrow$ and $\downarrow\uparrow$ DWs to move in the *same* direction and with the *same* speed ($\mathbf{v}_{\uparrow\downarrow} = \mathbf{v}_{\downarrow\uparrow}$), thus resulting in no net change in the overall magnetization, thus, no switching. The external magnetic field $\boldsymbol{H}_{\boldsymbol{x}}$ along the current direction $\boldsymbol{J}$ changes the relative orientation of the central DW moments, causing $\mathbf{v}_{\uparrow\downarrow}\neq\mathbf{v}_{\downarrow\uparrow}$ and enabling $+\boldsymbol{M}$ with one polarity and $-\boldsymbol{M}$ with the opposite polarity of current. Thus, the external field $\boldsymbol{H}_{\boldsymbol{x}}$ breaks the degeneracy of up-down and down-up DWs with regard to the SOT, and causes unequal DW motion that accomplishes switching, even for nanostructures [25]. Simulation using Eq. (1) reveals these essential results, including the necessity of an external field $\boldsymbol{H}_{\boldsymbol{x}}$ [23–26].

To date, SOT switching and the validity of Eq. (1) have been extensively studied only in HM/FM/I with *one* HM layer, involving spin current of one spin index $\boldsymbol{\sigma}$. Since the strengths a and b of the two SOT terms in Eq. (1) scale with θ_{SH}, efficient switching relies on a HM with a large θ_{SH}, such as Pt or W, whose main contrast lies in the opposite sign of θ_{SH} and the opposite SOT. In this work, we experimentally explore the implications of Eq. (1) by employing a *second* HM with an opposite spin index $-\boldsymbol{\sigma}$, such as Pt/W/CoFeB/MgO, as shown in Fig. 1(d). Since the two SOT terms are linear in $\boldsymbol{\sigma}$, the second HM with an opposite θ_{SH} would generate a pure spin current of opposite $\boldsymbol{\sigma}$. This should be expected to only reduce the net spin current and the associated SOT, resulting in a larger switching current density. With a sufficiently thick second HM, the net spin current and SOT of the HM bilayer complex would vanish, resulting in no current switching. In short, the effect of the second HM with opposite θ_{SH} is trivial and counterproductive as LLG simulation of Eq. (1) readily predicts. Contrary to conventional predictions, we observe effective SOT switching in Pt/W/CoFeB/MgO heterostructures. Not only is a net SOT evident in this material with nominally opposing SOTs, current induced switching occurs without any superimposed magnetic field, i.e., zero-field switching (ZFS), a feat that has eluded all HM/FM/I with a single HM. These results suggest a hitherto unknown mechanism due to *competing* spin currents that enables ZFS.

We used magnetron sputtering with normal incidence for the fabrication of the multilayers, except the W layer, which was made by oblique (off-axis) sputtering to capture the β-W phase. The direction of oblique sputtering also defines an important in-plane structural symmetry within W/CoFeB/MgO, with CoFeB as $Co_{40}Fe_{40}B_{20}$, in which the direction perpendicular to the off-axis direction is denoted as $\alpha = 0°$ and 180°. All the films were deposited on Si/SiO_2 substrate. The multilayers were then annealed in vacuum at 300 °C for 1 h to acquire the PMA of CoFeB. We use optical lithography to pattern multilayers into Hall bar structures, where the current channel is 20 μm(width)× 120 μm(length) and the voltage channel width of 10 μm, with the current direction along various directions specified by α. The oblique sputtered W layer has a thickness difference of about 1 nm over a lateral distance of 3 cm. The W thickness variation in the actual samples is within 10^{-3} nm, i.e., indistinguishable from a uniform layer.

We first discuss the results of Hall bars patterned in the direction of $\alpha = 0°$. The results of W(1)/CoFeB(1)/MgO(2) (in nm) are shown in Figs. 1(b) and 1(c). The AHE loops are centered at $\mu_0 H_z = 0$, regardless of the current value [Fig. 1(b)]. Consistent with the SOT switching phenomena, current induced switching of this device requires an external field $\mu_0\boldsymbol{H}_x$, where $+\mu_0 H_x$ (parallel to $+I$) leads to the $+M$ state at large $+I$, and the opposite for $-\mu_0 H_x$ [Fig. 1(c)]. However, the results of

Pt(3.8)/W(1)/CoFeB(1)/MgO (in nm), are very different. The AHE loops of Pt/W/CoFeB/MgO are distinctively off center with the loop shifts to one side [Fig. 1(e)] as if under a perpendicular field $\mu_0\boldsymbol{H}_\perp$, which increases linearly with current density J (See Supplemental Material II [15] for AHE of Pt/W/CoFeB/MgO devices). At a sufficiently large current, purely electrical switching occurs at zero field [Fig. 1(f)], i.e., ZFS. In fact, this sample continues to exhibit the same SOT switching under modest fields $\mu_0\boldsymbol{H}_x$ of up to about ± 10 mT. The switching current density between samples is similar, although the switching current in W/CoFeB/MgO [Fig. 1(c)] is smaller than that in Pt/W/CoFeB/MgO [Fig. 1(f)] due to different metal layer thicknesses.

To determine the relative contributions of Pt and W, we measured a series of samples of Pt(3)/W($t_W = 0.7$–1.6)/CoFeB(1)/MgO with a constant Pt(3) layer and various thicknesses of the W layer. As shown in Fig. 2(a), ZFS (solid symbols), each with a sizable $\mu_0\boldsymbol{H}_\perp$, has been observed in the range of about $0.7 < t_\mathrm{W} < 1.3$ nm. Samples outside this thickness range (open symbols) do not exhibit ZFS. In another series, we varied the Pt layer thickness in Pt($t_\mathrm{Pt} = 1.5$–4.5)/W(1)/CoFeB(1)/MgO and

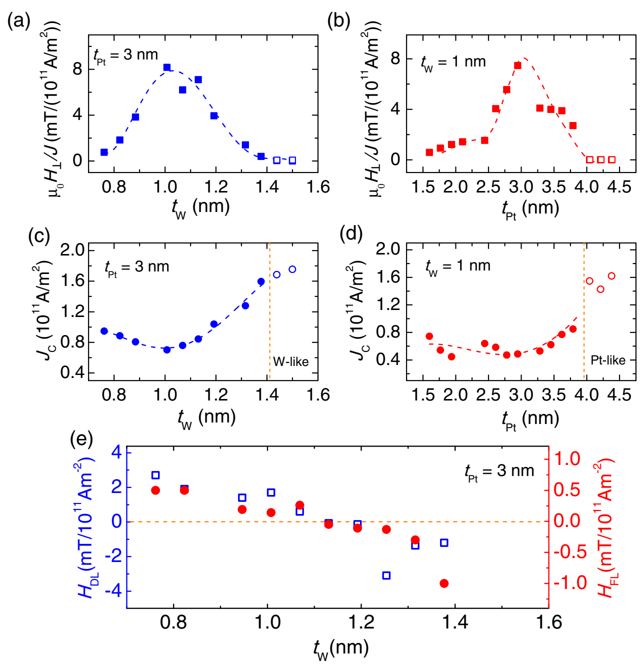

FIG. 2. SOT switching dependence on Pt and W thickness in Pt/W/CoFeB/MgO. In Pt(3)/W(t_W)/CoFeB(1)/MgO(1.8) with a fixed $t_\mathrm{Pt} = 3$ nm (a) $\mu_0\boldsymbol{H}_\perp/J$ and (c) switching density J_C. In Pt(t_Pt)/W(1)/CoFeB(1)/MgO(1.8) with a fixed $t_\mathrm{W} = 1$ nm, (b) $\mu_0\boldsymbol{H}_\perp/J$, and (d) J_C. In (c) and (d) the solid and open symbols are for $\mu_0 H_x = 0$ and 7 mT, respectively. (e) H_FL (solid circles) and H_DL (open squares) obtained from harmonic measurements for Pt(3.0)/W(t_W)/CoFeB(1)/MgO(1.8). These two series show Pt(3)/W(1.1)/CoFeB(1)/MgO(1.8) has the maximal $\mu_0\boldsymbol{H}_\perp/J$, minimal J_C, and $H_\mathrm{FL} \approx 0$, and $H_\mathrm{DL} \approx 0$.

observed ZFS with $1.5 < t_\mathrm{Pt} < 3.8$ as shown in Fig. 2(b). The ratio $\mu_0\boldsymbol{H}_\perp/J$, measures the efficiency of ZFS. As shown in Figs. 2(a) and 2(b), the $\mu_0\boldsymbol{H}_\perp/J$ value varies systematically with t_W and t_Pt with a maximal $\mu_0\boldsymbol{H}_\perp/J$ of 8 mT/(10^{11} A/m^2) occurring at Pt(3)/W(1)/CoFeB(1)/MgO from the two series. There is no ZFS with $\mu_0\boldsymbol{H}_\perp/J \approx 0$ and switching requires $\mu_0\boldsymbol{H}_x$ as in HM/FM/I. When the conventional SOT reduces [Fig. 2(e)], J_c dose not increase [Fig. 2(c)]. In fact, J_c has the lowest value in Pt(3)/W(1)/CoFeB(1)/MgO, the structure with robust ZFS and maximal $\mu_0\boldsymbol{H}_\perp/J$. For ZFS, the thicknesses of W ($0.8 < t_\mathrm{W} < 1.3$) are smaller than those of Pt ($1.5 < t_\mathrm{Pt} < 3.8$), because of the higher spin current injection efficiency from the W layer, which is in contact with the CoFeB layer. One might suspect that the second HM of Pt in Pt/W/CoFeB/MgO may alter the DMI, or cause other effects from the additional Pt/W interface. We note the DMI constants of W/CoFeB and Pt/CoFeB have the same sign and similar values [27–29].

We have also performed harmonic measurements [30–32] to quantitatively measure the effective H_DL and H_FL, through $H_{\mathrm{DL(FL)}} = 2[(dV_{2\omega})/(dH_{x(y)})]/[(d^2V_\omega)/(d^2H_{x(y)})]$, where $\mathrm{V}_{\omega,2\omega}$ are first and second harmonic Hall signal, $H_{x,y}$ are in-plane magnetic field along and perpendicular to the current direction. The results of Pt(3)/W($t_W = 0.7$–1.6)/CoFeB(1)/MgO are shown in Fig. 2(e). First of all, both SOTs in Pt/W/CoFeB/MgO are about 1 order of magnitude smaller than those with W and Pt alone [26,27], reflecting the reduced net spin current, consistent with conventional SOT phenomenology. Both $\boldsymbol{\tau}_\mathbf{FL}$ and $\boldsymbol{\tau}_\mathbf{DL}$ vary systematically with t_W from positive to negative as t_W increases. Importantly, both $\boldsymbol{\tau}_\mathbf{FL}$ and $\boldsymbol{\tau}_\mathbf{DL}$ cross zero at about $t_\mathrm{W} = 1$ nm. Thus, the most efficient ZFS switching occurs in Pt(3)/W(1)/CoFeB(1)/MgO, where all the key quantities for conventional SOTs, including $\boldsymbol{\tau}_\mathbf{FL}$, $\boldsymbol{\tau}_\mathbf{DL}$, and the effective θ_SH, are *vanishingly* small. This indicates that the ZFS in Pt(3)/W(1)/CoFeB/MgO is not adequately captured by the conventional SOT mechanism whose strength is evaluated by $\boldsymbol{\tau}_\mathbf{FL}$ and $\boldsymbol{\tau}_\mathbf{DL}$, but instead by a new mechanism, identified by $\mu_0\boldsymbol{H}_\perp/J$.

To reveal the magnetization switching under the electric current, we use magnetic optical Kerr effect (MOKE) imaging on Pt(2.5 nm)/W(1.0 nm)/CoFeB/MgO to directly observe magnetic domains and DW motion during current switching from $-M$ to $+M$ with $-I$ [Fig. 3(a)], and from $+M$ to $-M$ with $+I$ [Fig. 3(b)]. In these images, the up (down) or $+M$ ($-M$) domains have black (white) contrast. Under $-I$ of increasing magnitude, the images proceed in the order of 1, 2, 3, 4, 5, where the $+M$ domains expand asymmetrically. Because of the multiple domains, DW motions occur at multiple locations, with subsequent domain consolidation. The $\uparrow\downarrow$ DW on the right side moves opposite to the conventional current direction, while the $\downarrow\uparrow$ DW on the left side moves much slower. This disparity in the DW speeds of the two types of DWs, in the absence

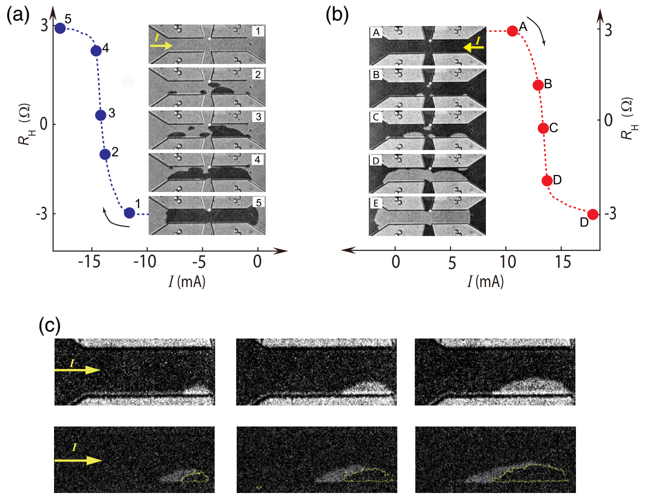

FIG. 3. MOKE images of current switching in Hall bar of Pt(2.5)/W(1.0)/CoFeB(1) for (a) increasing −I in the order of 1, 2, 3,… and (b) increasing +I in the order of A, B, C… (c) Images after successive current pulses asymmetrically enlarging the domains at one end. In the lower panel, the yellow boundaries show the domains just before the current pulse, illustrating the contribution of the one current pulse.

of a magnetic field, is the key feature of Pt/W/CoFeB/MgO that leads to ZFS. The reverse process is shown in Fig. 3(b) under $+I$ of increasing magnitude shown by the images in the order of A to E, and similar asymmetrical DW motion was observed. It is noted that, the DWs tend to expand as current increases (see Supplemental Material IV [15] for domain expansion under current), suggesting a perpendicular field associated with the current in Pt/W. By including the $\mu_0 \boldsymbol{H}_\perp / J$ in Eq. (1), together with the conventional SOT described by $\boldsymbol{M} \times (\boldsymbol{\sigma} \times \boldsymbol{M})$, the asymmetric motion of ↑↓ and ↓↑ DWs along current direction, thus the ZFS, can be well reproduced by LLG equation (see Supplemental Material IV [15] for the simulation of asymmetric domain wall motion, which including Refs. [26,28,33]).

We use current pulses of 11.8 mA in magnitude and 50 μs in width to reveal the consequence of each current pulse. In the top row of Fig. 3(c), we show the MOKE images of the same region after 3 successive current pulses. In the lower row we highlight in yellow the domain after the previous current pulse, revealing the asymmetrical domain growth from this current pulse. From these images one concludes that the highest DW speed, occurring at the tip of the down-up DW after each current pulse, is about 3 cm/s at this low current density. An increase in current density dramatically increases the DW speed as necessary for devices application [23,24].

We next discuss the ZFS switching anisotropy. In W/CoFeB/MgO, as in other HM/FM/I, the external field $\mu_0 \boldsymbol{H}_x$ along the current direction sets the switching sense of the $\pm M$ states as shown in Fig. 1(c). The current channel

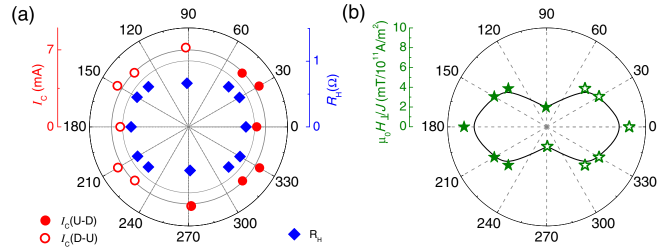

FIG. 4. Anisotropy of ZFS in Pt(3)/W(1.1)/CoFeB(1)/MgO(2) (in nm). (a) Angular dependence of the R_H values, I_C, and (b) $\mu_0 \boldsymbol{H}_\perp / J$ values, where the solid and open circles indicate magnetization switching from up to down and down to up, respectively.

may be patterned along any direction α within the CoFeB plane with no discernable difference. This isotropy is also realized in W/CoFeB/MgO samples with the oblique sputtered W layer. However, in Pt/W/CoFeB/MgO [Fig. 1(f)] that exhibits ZFS, current of opposite polarities gives the opposite states of $\pm \boldsymbol{M}$, thus with a distinct anisotropy. We patterned Pt/W/CoFeB/MgO with 10 μm channel width along different directions in the film plane, with $\alpha = 90°$ denoted as the off-axis sputtering direction. The angular dependence of the switching current is shown in Fig. 4(a), where the switching current mid-points for up-to-down and down-to-up are denoted as $I_C(U-D)$ (solid circles) and $I_C(D-U)$ (open circles), respectively. The remnant Hall resistance $R_H(0)$ that measures the degree of reversal is also shown. The angular dependence of $I_C(U-D)$, $I_C(D-U)$, and $R_H(0)$ shows a twofold symmetry with $\alpha = 0°$ as the symmetry axis. Deterministic switching occurs with nearly the same switching current of ± 6.7 mA ($J_c = 1.3 \times 10^{11}$ A/m^2) within a wide range of angle of about $\pm 60°$ centered at $\alpha = 0°$, and with the opposite M at $\alpha = 180°$. In contrast, only partial switching with a smaller $R_H(0)$, requiring a larger current of ± 7.1 mA ($J_c = 1.4 \times 10^{11}$ A/m^2), occurs near the perpendicular direction of $\alpha = 90°$ and 270°. The anisotropy axis is likely set by the oblique sputtering direction for the W layer. Off-axis sputtering is known to promote grain growth in the oblique direction, which causes the in-plane anisotropy [34,35].

In addition to Pt/W/CoFeB/MgO, we have also observed ZFS in Pt/Ta/CoFeB/MgO but not in Ta/W/CoFeB/MgO. Since Ta and W both have negative $\theta_{\rm SH}$ and Pt has positive $\theta_{\rm SH}$, these results further reaffirm the essential feature of two spin currents with opposite $\boldsymbol{\sigma}$ rather than multilayer structure To further demonstrate the essential features of two spin currents of opposite spin index, in Pt/W/CoFeB/MgO with ZFS, we insert a 1-nm Au layer between Pt and W as in Pt/Au/W/CoFeB/MgO, where the much weaker charge-to-spin conversion of Au effectively reduces the spin current from Pt [36,37]. As a result, ZFS no longer occurs, and switching requires a field. To address the Oersted field due to the charge current, we capped the Pt/W/CoFeB/MgO with Ta(1 nm)/Au(3 nm), the current through which would compensate the Oersted field from the bottom Pt/W. We found ZFS remains intact thus excluding Oersted field as a possible cause. These observations reaffirm the essential features of competing spin currents. We note a pure spin current, with a direction, a magnitude, and a spin index $\boldsymbol{\sigma}$, is *not* a vector. But in the present model of SOT, the effect of the spin current has been incorporated into a spin flux vector with direction $\boldsymbol{\sigma}$ and a magnitude that scales with θ_{SH}, as in the fieldlike torque ($a\boldsymbol{M} \times \boldsymbol{\sigma}$) and the anti-damping-like torque [$b\boldsymbol{M} \times (\boldsymbol{\sigma} \times \boldsymbol{M})$] in Eq. (1). To accomplish ZFS one needs create additional in-plane anisotropy on magnetic unit through geometrical shape [16–18] or exchange bias [19,20]. We show in this work, the competing spin currents can also facilitate a new mechanism, experimentally revealed as $\mu_0 \boldsymbol{H}_\perp \propto J$, that causes asymmetric motion of up-down and down-up DWs along current direction, and performs ZFS at sufficiently large current.

In summary, we demonstrate a novel switching mechanism via two spin currents of opposite spin indices in Pt/W/CoFeB/MgO and similar structures. Instead of merely canceling the spin current and SOT as the present model would indicate, we show that the competing spin currents generate an effective SOT with an effective perpendicular field that can switch a PMA layer without any applied magnetic field. We show that the present model of SOT does not provide a viable scheme for multiple spin currents, a new avenue for magnetization switching and DW motion.

4 This work was supported by the U.S. Department of Energy, Basic Energy Science, Award Grant No. DE-SC0009390. Y. L. was supported in part by STARnet, a SRC program sponsored by MARCO and DARPA. Q. M. was supported in part by SHINES, an EFRC funded by the U.S. DOE Basic Energy Science Award No. SC0012670. Q. M. thanks Weiwei Lin for helpful discussions on magnetization switching related to domain wall motion.

Q. M. and Y. L. contributed equally to this work.

---

*Corresponding author.
qma7@jhu.edu
†Corresponding author.
clchien@jhu.edu

[1] C. Chappert, A. Fert, and F. N. Van Dau, Nat. Mater. **6**, 813 (2007). 5
[2] N. Locatelli, V. Cros, and J. Grollier, Nat. Mater. **13**, 11 (2014).
[3] J. C. Slonczewski, J. Magn. Magn. Mater. **159**, L1 (1996); **195**, L261 (1999).
[4] L. Berger, Phys. Rev. B **54**, 9353 (1996); J. Appl. Phys. **81**, 4880 (1997).
[5] J. C. Sankey, Y.-T. Cui, J. Z. Sun, J. C. Slonczewski, R. A. Buhrman, and D. C. Ralph Nat. Phys. **4**, 67 (2008).
[6] S. S. P. Parkin, M. Hayashi, and L. Thomas, Science **320**, 190 (2008).
[7] A. Manchon and S. Zhang, Phys. Rev. B **79**, 094422 (2009).
[8] M. D. Stiles and Z. Zangwill, Phys. Rev. B **66**, 014407 (2002). 6
[9] V. P. Amin and M. D. Stiles, Phys. Rev. B **94**, 104419 (2016).
[10] I. M. Miron, K. Garello, G. Gaudin, P.-J. Zermatten, M. V. Costache, S. Auffret, S. Bandiera, B. Rodmacq, A. Schuhl, and P. Gambardella Nature (London) **476**, 189 (2011).
[11] L. Liu, O. J. Lee, T. J. Gudmundsen, D. C. Ralph, and R. A. Buhrman, Phys. Rev. Lett. **109**, 096602 (2012).
[12] L. Liu, C.-F. Pai, Y. Li, H. W. Tseng, D. C. Ralph, and R. A. Buhrman Science **336**, 555 (2012).
[13] Q. Hao and G. Xiao, Phys. Rev. Applied **3**, 034009 (2015).
[14] C. Zhang, M. Yamanouchi, H. Sato, S. Fukami, S. Ikeda, F. Matsukura, and H. Ohno J. Appl. Phys. **115**, 17C714 (2014).
[15] See Supplemental Material at http://link.aps.org/supplemental/10.1103/PhysRevLett.000.000000 for [brief description]. 7
[16] G. Yu *et al.* Nat. Nanotechnol. **9**, 548 (2014).
[17] L. Youa, O. Lee, D. Bhowmik, D. Labanowski, J. Hong, J. Bokor, and S. Salahuddin Proc. Natl. Acad. Sci. U.S.A. **112**, 10310 (2015).
[18] C. K. Safeer, E. Jué, A. Lopez, L. Buda-Prejbeanu, S. Auffret, S. Pizzini, O. Boulle, I. Mihai Miron, and G. Gaudin Nat. Nanotechnol. **11**, 143 (2016).
[19] S. Fukami, C. Zhang, S. DuttaGupta, A. Kurenkov, and H. Ohno Nat. Mater. **15**, 535 (2016).
[20] Y.-C. Lau, D. Betto, K. Rode, J. M. D. Coey, and P. Stamenov Nat. Nanotechnol. **11**, 758 (2016).
[21] O. J. Lee, L. Q. Liu, C. F. Pai, Y. Li, H. W. Tseng, P. G. Gowtham, J. P. Park, D. C. Ralph, and R. A. Buhrman, Phys. Rev. B **89**, 024418 (2014).
[22] C. O. Avciet *et al.*, Phys. Rev. B **89**, 214419 (2014).
[23] S. Emori, U. Bauer, S.-M. Ahn, E. Martinez, and G. S. D. Beach, Nat. Mater. **12**, 611 (2013).
[24] P. P. J. Haazen, E. Murè, J. H. Franken, R. Lavrijsen, H. J. M. Swagten, and B. Koopmans, Nat. Mater. **12**, 299 (2013).
[25] M. Baumgartner *et al.*, Nat. Nanotechnol. **12**, 980 (2017).
[26] A. V. Khvalkovskiy, V. Cros, D. Apalkov, V. Nikitin, M. Krounbi, K. A. Zvezdin, A. Anane, J. Grollier, and A. Fert, Phys. Rev. B **87**, 020402(R) (2013).
[27] K. Di, V. L. Zhang, H. S. Lim, S. C. Ng, M. H. Kuok, X. Qiu, and H. Yang, Appl. Phys. Lett. **106**, 052403 (2015).
[28] A. K. Chaurasiya, C. Banerjee, S. Pan, S. Sahoo, S. Choudhury, J. Sinha, and A. Barman, Sci. Rep. **6**, 32592 (2016).
[29] I. Gross, H. Keller, R. K. Kremer, J. Kohler, H. Luetkens, T. Goko, A. Amato, and A. Bussmann-Holder, Phys. Rev. B **94**, 064413 (2016). 8
[30] J. Kim, J. Sinha, M. Hayashi, M. Yamanouchi, S. Fukami, T. Suzuki, S. Mitani, and H. Ohno, Nat. Mater. **12**, 240 (2013).
[31] J. Cho *et al.*, Nat. Commun. **6**, 7635 (2015).

[32] K. Garello, I. M. Miron, C. O. Avci, F. Freimuth, Y. Mokrousov, S. Blügel, S. Auffret, O. Boulle, G. Gaudin, and P. Gambardella, Nat. Nanotechnol. **8**, 587 (2013).

[33] Q. L. Ma, S. Iihama, T. Kubota, X. M. Zhang, S. Mizukami, Y. Ando, and T. Miyazaki Appl. Phys. Lett. **101**, 122414 (2012).

[34] R. N. Tait, T. Smy, and M. J. Brett J. Vac. Sci. Technol. A **10**, 1518 (1992).

[35] R. D. McMichael, C. G. Lee, J. E. Bonevich, P. J. Chen, W. Miller, and W. F. Egelhoff, J. Appl. Phys. **88**, 5296 (2000).

[36] M. Isasa, E. Villamor, L. E. Hueso, M. Gradhand, and F. Casanova, Phys. Rev. B **91**, 024402 (2015).

[37] H. J. Zhang, S. Yamamoto, Y. Fukaya, M. Maekawa, H. Li, A. Kawasuso, T. Seki, E. Saitoh, and K. Takanashi, Sci. Rep. **4**, 4844 (2015).